Point-Mass Model for Nano-Patterning Using Dip-Pen nanolithography

Seok-Won Kang and Debjyoti Banerjee*

*Department of Mechanical Engineering, Texas A&M University
College Station, TX 77843-3123, USA, dbanerjee@tamu.edu

ABSTRACT

Micro-cantilevers are frequently used as scanning probes and sensors in micro-electromechanical systems (MEMS). Usually micro-cantilever based sensors operate by detecting changes in cantilever vibration modes (e.g., bending or torsional vibration frequency) or surface stresses - when a target analyte is adsorbed on the surface. The catalyst for chemical reactions (i.e., for a specific analyte) can be deposited on micro-cantilevers by using Dip-Pen Nanolithography (DPN) technique. In this study, we simulate the vibration mode in nano-patterning processes by using a Point-Mass Model (or Lumped Parameter Model). The results from the simulations are used to derive the stability of writing and reading mode for a particular driving frequency during the DPN process. In addition, we analyze the sensitivity of the tip-sample interaction forces in fluid (ink solution) by utilizing the Derjaguin-Muller-Toporov (DMT) contact theory.

Keywords: Derjaguin-Muller-Toporov, contact theory, vibration, beam theory

1 INTRODUCTION

Dip-pen Nanolithography (DPN) is a popular nano-patterning technique for deposition of materials onto a substrate using the scanning probe of an atomic microscope (AFM). To ensure repeatability for batch production by DPN using an AFM instrument, it is very important to control and detect the reflected laser signals from the probe surface for monitoring the position and the vibration of the tip. The dynamic behavior depends on various parameters such as the tip-sample interactions, operational environments, material properties or geometrical configuration of the scanning probe. The nonlinear dynamical characteristics of the AFM tip caused by the tip-sample interactions have been investigated in various studies [1-8].

The lumped-parameter models of conventional rectangular micro-cantilever probes fall into two categories: (A) Point-mass models [1-3]; and (B) Discretized models [4-8], that are derived from continuous beam equations. The former typically assumes that regardless of the cantilever geometry, the probe stiffness of the each eigenmode can be scaled by taking the static bending stiffness of the cantilever which relates its tip deflection to a static point load at the free end and scaling factor of each mode. On the other hand, it is not easy to find different choices of eigenmode scaling and normalization to get an equivalent mass and stiffness for higher-order modes. The later requires a number of matrix calculations. However, it can be used to explain the higher-order vibration modes and obtain the exact results for very small vibration amplitudes.

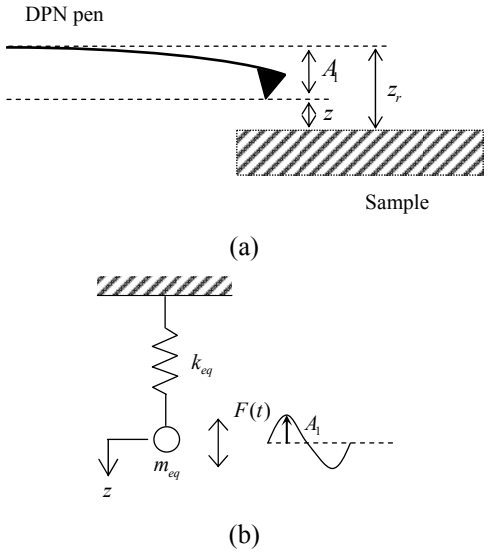

Figure 1: Equivalent point-mass representation of a cantilever oscillating in a single eigenmode

As shown in Fig. 1, for a fixed sample we can assume that cantilever bends as if a static point load has been applied at the cantilever's free-end. Using the corresponding static stiffness we can derive a single degree of freedom point-mass model.

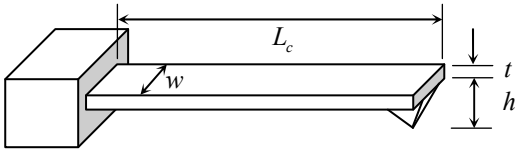

Figure 2: Schematic of DPN Pen cantilever with uniform and rectangular cross section

In DPN during the deposition step the scanning probe tip is moved very slowly in contact with the substrate enabling the flow of ink materials from the tip to the sample. For characterization of the deposited features frictional force variations on the sample are scanned by oscillating

the tip laterally at a faster traverse rate over a designated area on the substrate, resulting in transverse and longitudinal vibration modes to be excited due to the lateral oscillations. The DPN pen cantilever used in this study is a rectangular elastic beam as shown in Fig. 2. The cantilever has a length L_c, thickness t, width w and tip height h. In this study we calculate the different vibration modes that are generated during the writing process for material deposition (flexural vibration) and during the reading process for characterization of the deposited material (lateral vibration), using a Si_3N_4 (Silicon Nitride) pen tip over a gold (Au) coated sample.

2 MODELING OF THE SYSTEM

2.1 Point-mass model

In this study we explore the equivalent point-mass model for a uniform, rectangular, microcantilever scanning probe, as shown in Fig. 2. The micro-cantilever is modeled as a driven, damped harmonic oscillator given by [1-3]

$$m_{eq}\ddot{z} + b\dot{z} + k_{eq}(z - z_r) = F_0\cos(\omega t) + f_{TS}(t) \tag{1}$$

where z is the cantilever position with respect to the surface, $F_0=k_{eq}A_1$ is the driving force (A_1 is the driving amplitude), ω is the driving frequency, $f_{TS}(t)$ is the tip-sample interaction force and $b=m_{eq}\omega_n/Q$ is the damping coefficient, where ω_n is the natural frequency and Q is the quality factor. It is assumed that when the microcantilever is excited near the flexural resonance for mode numer "i", an unique equivalent masses m_{eq} and stiffness $k_{N,eq}$ can be be used to represent the resulting dynamics of the system and these parameters can be systematically determined by equating the kinetic energy (T) and potential energy (V) of a continuous probe to that of an appropriate point-mass model [2].

$$T = \frac{1}{2}\int_0^{L_c}\rho_c\dot{w}(x,t)^2\,dx = \frac{1}{2}m_{eq}^i\dot{q}^2 \rightarrow m_{eq} = \frac{1}{4}m_c \tag{2}$$

$$V = \frac{1}{2}\int_0^{L_c}E_cI_c\ddot{w}(x,t)^2\,dx = \frac{1}{2}k_{eq}^i q^2 \rightarrow k_{N,eq} = \frac{1}{12}k_c\alpha_i^4 \tag{3}$$

where $m_c=\rho_cL_c$ is the total mass of the cantilever, $k_c=3E_cI_c/L_c^3$ and α_i is the ith solution of the dispersion relation, $cos(\alpha)cosh(\alpha)+1=0$, such that the resonance frequency $\omega_{i,n}^2=E_cI_c\alpha_i^4/\rho_cL_c^4$ (α_1=1.875, α_2=4.694 and α_3=7.855).

In DPN, the deposited features are characterized by the Lateral Force Microscopy (LFM). The lateral force that is generated when the tip is in contact with the sample in scanning mode, causes both lateral and torsional deflection of the tip. The lateral and torsional spring constants corresponding to the normal spring constant are defined as follows [9-10]:

$$k_{lat} = k_{N,eq}\left(\frac{w}{t}\right)^2 \tag{4}$$

$$k_{tor} = k_{N,eq}\frac{1}{2}\left(\frac{L_c}{h}\right)^2 \tag{5}$$

The effective spring constant for the lateral deflection due to frictional force can be defined as coupling of lateral and torsional spring constants in series [9].

$$\frac{1}{k_{L,eff}} = \frac{1}{k_{lat}} + \frac{1}{k_{tor}} \tag{6}$$

Vibration analysis based on point-mass model should be independently analyzed for both normal and lateral modes since the point-mass model is valid only for one-directional vibration mode.

2.2 Tip-sample interaction force

The pen probe is subject to three kinds of tip-sample interaction forces: remote attraction (van der Walls for $z \geq d_0$), repulsion (ionic and Pauli for $z \leq d_0$), and contact attraction (i.e. adhesion – governed by material characteristics). These interactions are represented by Eq. 7. In DPN process the adhesion force (i.e., so called pull off force arising from capillary bridge formed between tip and sample due to condensation of water droplet from ambient humidity) enables the tip to maintain constant contact with sample (or substrate) and overcome the repulsive forces due to Van der Waals forces or due to hydrogen bonds.

$$f_{ts}(t) = \begin{cases} \dfrac{-A_HR}{6z^2} & for \quad z \geq d_0 \\ \dfrac{-A_HR}{6z^2} + \dfrac{4}{3}E^*\sqrt{R}(d_0 - z)^{3/2} & for \quad z \leq d_0 \end{cases} \tag{7}$$

with

$$\frac{1}{E^*} = \frac{\left(1-\nu_t^2\right)}{E_t} + \frac{\left(1-\nu_s^2\right)}{E_s} \tag{8}$$

where A_H is the Hamaker constant, R is the tip radius, d_0 is the intermolecular distance between tip and sample and E^* is the effective elasticity, where E_c, ν_c and E_s, ν_s are the elastic module and Poisson's ratios of the tip and sample, respectively. The Derjaguin-Muller-Toporov (DMT) model is valid for stiff tips and samples with low adhesion forces. This model is commonly used in AFM studies to represent silicon probe tips [11]. The contact mode of AFM is typically utilized in the DPN process. In the contact region (gray colored region in Fig. 3), the tip-sample force based on DMT model can be simplified as:

$$f_{N,TS}(t) = \frac{4}{3}E^*\sqrt{R}(d_0 - z)^{3/2} \quad for \quad z \leq d_0 \tag{9}$$

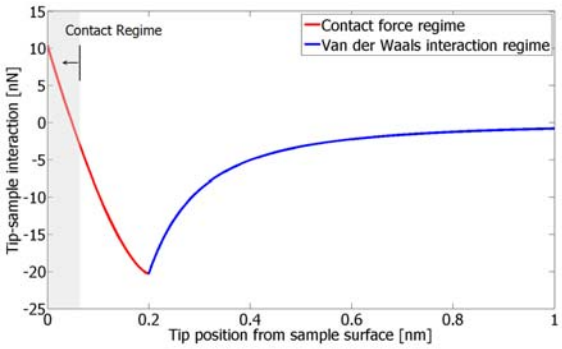

Figure 3. Tip-sample interaction force

If the tip is in contact with the sample for a fixed duration, (where we assume that the motion of the tip has a sinusoidal profile) then the indentation depth is also sinusoidal during the duration of contact. In lateral vibration (scanning) mode, according to the Hertzian contact theory, the tip-sample interaction forces at the tangential (and lateral) directions are a function of the normal contact force [6].

$$f_{T,TS}(t) = f_{L,TS}(t) = 8G^*\left(\frac{3Rf_{N,TS}}{4E^*}\right)^{1/3} \quad for \quad z \le d_0 \tag{10}$$

with

$$\frac{1}{G^*} = \frac{(2-\nu_t)}{G_t} + \frac{(2-\nu_s)}{G_s}, \text{ where } G = \frac{E}{2(1+\nu)} \tag{11}$$

The analytical evaluation of f_{TS} shown in Eq. 9 and 10 contains incomplete elliptical functions. Calculating the incomplete elliptical functions takes a long time. For the purpose of faster calculation, it is usually approximated using Fourier Transform or Linearization [12-13]. In this calculation, we used linearization based on Taylor series expansion.

3 NUMERICAL SIMULATION

Finite Element Analysis (FEA) is typically used to simulate the structural dynamics of continuous models of cantilever. In this study, the natural frequency is calculated by performing numerical simulations using Finite Element Analyses (FEA) that is implemented on a commercial FEA tool (ANSYS®). The harmonic simulations are performed using the SOLID45 element and by implementing the node-to-surface contact scheme. Figure (4) depicts a representative geometry for performing the simulations. The normal contact stiffness k_n is estimated from the contact theory as [14,15]:

$$k_n = \frac{\partial F_{st}}{\partial d} = (6RE^{*2}F_N)^{1/3} \tag{12}$$

A similar expression can be derived for the lateral stiffness, k_l, by assuming negligible slip between the tip and the sample [15,16]:

$$k_l = \frac{k_n}{E^*}\left[\frac{\left(1-\frac{\nu_s}{2}\right)(1+\nu_s)}{E_s} + \frac{\left(1-\frac{\nu_t}{2}\right)(1+\nu_t)}{E_t}\right]^{-1} \tag{13}$$

$$\approx k_n \frac{1-\nu}{1-\frac{\nu}{2}}$$

where, the approximate relation $k_l \approx 0.9k_n$ applies to an incompressible tip. The normal and lateral excitations were exerted at the end of the pen tip for performing the harmonic simulations using the continuous models.

4 RESULTS AND DISCUSSION

Numerical simulations of theoretical models were performed and analyzed with Matlab (Mathworks Inc., Natick, MA) using parameters summarized in Table (1).

Table 1: Constants and properties of the Si_3N_4 microcantilever and *Au* sample used in numerical computation.

Description	Value
Tip radius	$R = 15nm$
Cantilever length	$L = 200\mu m$
Cantilever width	$b = 45\mu m$
Cantilever thickness	$h = 600nm$
Cantilever material density	$\rho_c = 3100kg/m^3$
Cantilever Young's modulus	$E_c = 210GPa$
Cantilever Poisson ratio	$\nu_c = 0.22$
Sample material density	$\rho_s = 19320kg/m^3$
Sample Young's modulus	$E_s = 80GPa$
Sample Poisson ratio	$\nu_s = 0.4$
Effective elastic modulus	$E^* = 66.53GPa$
Static bending stiffness	$k = 0.064N/m$
1st natural frequency	$f_1 = 19.358$
Q factor (in air)	$Q = 80.0$
Hamaker constant (Si_3N_4-Au)	$A_H = 32.5\times10^{-20}J$
Intermolecular distance	$a_0 = 2.0Å$

The natural frequencies of cantilever in free flexural vibration mode obtained from theoretical calculation and ANSYS simulation are in good agreement, as shown in Table 2. In Table 2, the differences between simulation results and experimental data can be due to variations in geometrical features in the experiments due to manufacturing tolerances. The data sheet for the scanning probes suggests a natural frequency of 27 kHz, which is probably the experimentally measured value of one sample cantilever, and the difference due to manufacturing

tolerances is potentially in the nominal range of *9~17 kHz* [17]. Fig. 5 shows the estimation of natural frequencies from point-mass model when we consider the tip-sample interactions. Originally, the point-mass model can usually be adopted for the investigation of vibrations when cantilevers are excited near a resonance frequency. Also, this cannot deflect the higher-order modes. For the small vibration amplitudes, we should use the FEA models.

show good agreement as follows:

Table 2: Resonance frequency in free-flexural vibration.

Description	Value [*kHz*]
Theoretical Calculation	*19.358*
ANSYS Mode Analysis	*19.349*
Data Sheet/ Experimental Measured Value (NanoInk, Inc.)	*27*

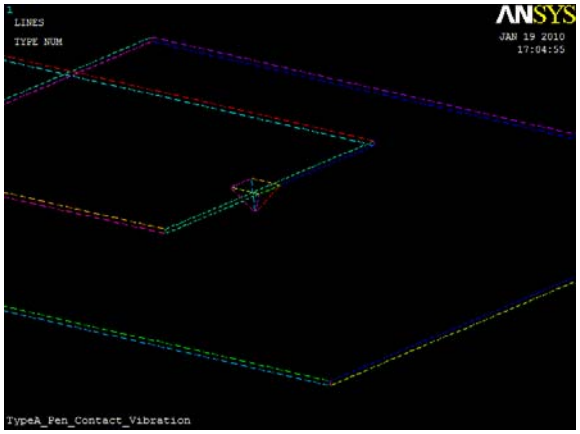

Figure 4: Solid model of the micro-cantilever.

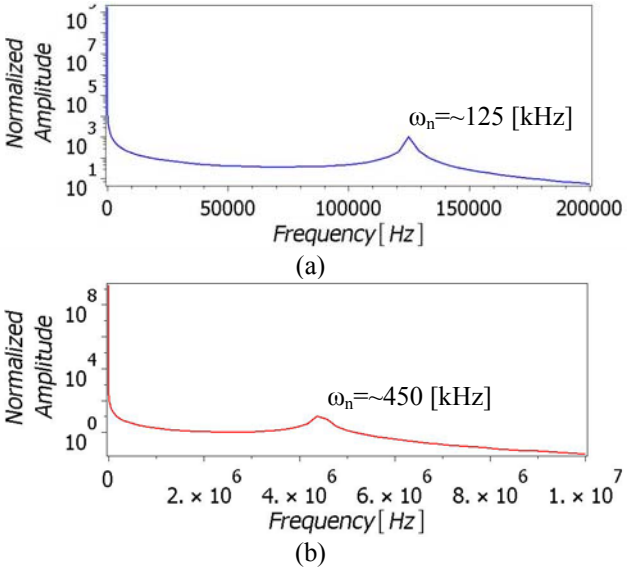

Figure 5: Natural frequency estimated by the theoretical models (a) normal (b) lateral-directions

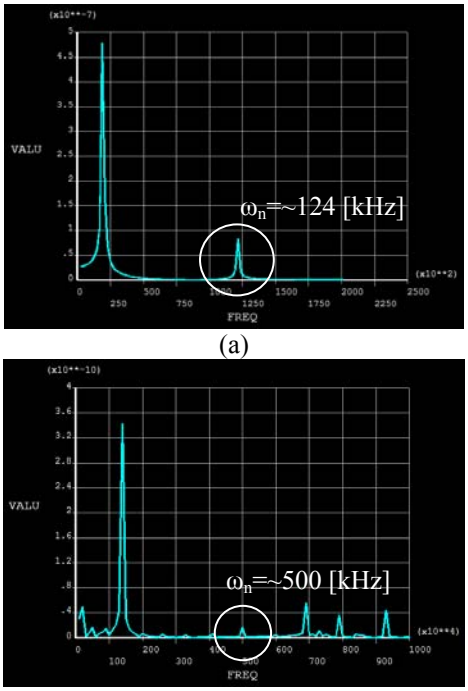

Figure 6: Simulation results of FEA model (a) normal (b) lateral-directions

In Fig. 6, the peak represented by the solid line corresponds to the natural frequency of the cantilever under ambient conditions (i.e., resonance in air). When the interaction with the Au coated substrate is considered, resonant frequencies in flexural and lateral modes are obtained based on both models and the peak is increased by approximately ~125 kHz and ~500 kHz (the second peak) as shown in Fig.5 and Fig. 6. The tip-sample interaction force acts as an additional spring resulting in higher value of the peak. Better agreement between the simulations was observed in the flexural mode rather than in the lateral mode. Hence for the lateral vibrations both lateral and torsional modes are significant.

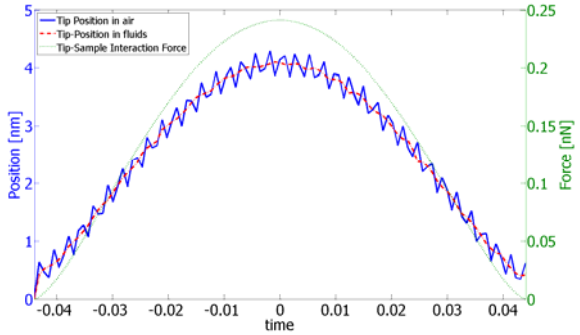

Figure 6: Tip position and Force in one oscillation cycle at the driving frequency *ω=1 [Hz]*.

Usually, the pen tip and sample interactions in DPN are modified due to presence of condensed water droplets resulting in tip-substrate interactions in fluid environments.

This operation differs significantly from that in air. The major difference between vibrations in air and in fluids is due to the decrease in the quality factor (Q) of the cantilever [3,18]. In air, Q of DPN pen cantilever is normally on the order of ~100-400, whereas in fluids, it is of the order of ~1-5. This is primarily due to the increased hydrodynamic damping in liquids in comparison with air. Fig.6 reveals the attenuation of the vibration in fluids (i.e. for $Q=5$).

5 SUMMARY AND CONCLUSIONS

In this study we explored the vibration analysis between Si_3N_4 pen of uniform and rectangular cross section with a gold (Au) coated sample, using the Point-Mass Model and Continuous-Beam Model, respectively, as representative situations during the DPN process. The point-mass models are limited in that they cannot capture the higher-order vibrations and complex mechanisms occurring due to the coupling between different modes (i.e. flexural and lateral modes or lateral and torsional mdoes). Nevertheless, these models have been used often in vibration mode analysis of micro-cantilevers due to the low computational costs for parametric studies and the ease of implementation of these models for obtaining estimates of vibration modes in nonlinear dynamics. In this study, predictions from the point-mass model for the resonance frequency under the free vibration as well as the tip-sample interactions, are found to be in good agreement with the calculations performed using FEA simulations.

REFERENCES

[1] Zhihua Liu, Yongliang Yang, Yanli Qu, Zaili Dong, Wen J. Li and Yuechao Wang, "Vibration-Mode Based Real-Time Nanoimaging and Nanomanipulation," Proceedings of the 7th IEEE International Conference on Nanotechnology, August 2 - 5, 2007, Hong Kong, pp, 515-519.

[2] John Melcher, Shuiqing Hu, and Arvind Raman, "Equivalent point-mass models of continuous atomic force microscope probes," Applied Physics Letters, 91, 053101-1-053101-3, 2007.

[3] Justin Legleiter, Matthew Park, Brian Cusick, and Tomasz Kowalewski, "Scanning probe acceleration microscopy (SPAM) in fluids: Mapping mechanical properties of surfaces at the nanoscale," PNAS, 103, 13, 4813-4818, 2006.

[4] Tser-Son Wu, Win-Jin Chang, and Jung-Chang Hsu, "Effect of tip length and normal and lateral contact stiffness on the flexural vibration responses of atomic force microscope cantilevers," Microelectronic Engineering, 71, 15-20, 2004.

[5] S. I. Lee, S. W. Howell, A. Raman, and R. Reifenberger, "Nonlinear dynamics of Microcantilevers in tapping mode atomic force microsocopy: A comparison between theory and experiment," Physical Review B, 66, 2002, 115409-1-115409-10, 2002.

[6] Yaxin Song and Bharat Bhushan, "Simulation of dynamic modes of atomic force microsocopy using a 3D finite element model," Ultramicroscopy, 106, 847-873, 2006.

[7] F. Mokhtari-Nezhad, A.R. Saidi, and S. Ziaei-Rad, "Influence of the tip mass and position on the AFM cantilever dynamics: Coupling between bending, torsion and flexural modes," Ultramicroscopy, 109, 1193-1202, 2009.

[8] R. Arinero and G. Leveque, "Vibration of the cantilver in force modulation microscopy analysis by a finite element model," Review of Scientific instruments, 74, 1, 104-111, 2003.

[9] O. Pietrement, J.L. Beaudoin and M. Troyon, "A new calibration method of the lateral contact stiffness and lateral force using modulated lateral force microscopy," Tribology Letters, 7, 213-220, 1999.

[10] Charles A Clifford and Martin P Seah, "The determination of atomic force microscope cantilever spring constants via dimensional methods for nanomechanical analysis," Nanotechnology, 16, 1666-1680, 2005.

[11] B. V. Derjaguin, V. M. Muller and Yu. P. Toporov, "Effect of contact deformations on the adhesion of particles," Colloid Interface Science, 53, 314-326, 1975

[12] Robert W. Stark and Wolfgang M. Heckl, "Fourier transformed atomic force microscopy: tapping mode atomic force microscopy beyond the Hookian approximation," Surface Science, 457, 219-228, 2000.

[13] M. Balantekin and A. Atalar, "Power dissipation analysis in tapping-mode atomic force microscopy," Physical Review, 67, 193404-1193404-4, 2003.

[14] Pierre-Emmanuel Mazeran and Jean-Luc Loubet, "Normal and lateral modulation with a scanning force microscope, and an analysis: implication in quantitative elastic and friction imaging," Tribology Letters, 7, 199-212, 1999.

[15] M. A. Lantz, S. J. O'Shea, A. C. F. Hoole, and M. E. Welland, "Lateral stiffness of the tip and tip-sample contact in frictional force microscopy," Applied Physics Letters, 70, 118476-1-118476-3, 1997.

[16] K. L. Johnson, "Contact Mechanics," Cambridge University Press, 1985.

[17] Paul E. West, "Introduction to atomic force microscopy-Theory, practice and applications", 1st Ed., 2006.

[18] Sudipta Basak and Arvind Raman, "Dynamics of tapping mode atomic force microscopy in liquids: Theory and experiments," Applied Physics Letters, 91, 064107-1-064107-3, 2007.